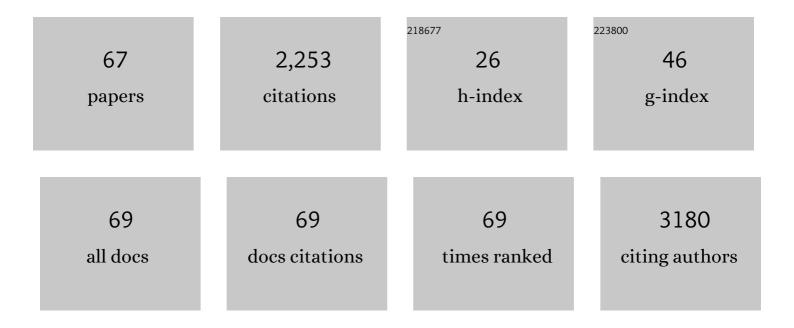
Yuhao Li, 掰ç§

List of Publications by Year in descending order

Source: https://exaly.com/author-pdf/12043995/publications.pdf Version: 2024-02-01



#	Article	IF	CITATIONS
1	Upconversion nanoparticles for the future of biosensing. , 2022, , 305-363.		Ο
2	Benzothiazole-decorated iridium-based nanophotosensitizers for photodynamic therapy of cancer cells. Dalton Transactions, 2022, 51, 3666-3675.	3.3	7
3	Fluorescent Imaging-Guided Chemo- and Photodynamic Therapy of Hepatocellular Carcinoma with HCPT@NMOFs-RGD Nanocomposites. International Journal of Nanomedicine, 2022, Volume 17, 1381-1395.	6.7	7
4	Quantitative hypoxia mapping using a self-calibrated activatable nanoprobe. Journal of Nanobiotechnology, 2022, 20, 142.	9.1	6
5	Near-Infrared Frequency Upconversion Luminescence Bioimaging Based on Cyanine Nanomicelles. ACS Applied Polymer Materials, 2022, 4, 5566-5573.	4.4	2
6	Dual-light triggered metabolizable nano-micelles for selective tumor-targeted photodynamic/hyperthermia therapy. Acta Biomaterialia, 2021, 119, 323-336.	8.3	25
7	Bistratal Au@Bi2S3 nanobones for excellent NIR-triggered/multimodal imaging-guided synergistic therapy for liver cancer. Bioactive Materials, 2021, 6, 386-403.	15.6	38
8	BSA-encapsulated cyclometalated iridium complexes as nano-photosensitizers for photodynamic therapy of tumor cells. RSC Advances, 2021, 11, 15323-15331.	3.6	14
9	Bat influenza vectored NS1-truncated live vaccine protects pigs against heterologous virus challenge. Vaccine, 2021, 39, 1943-1950.	3.8	7
10	Knockout of zebrafish colony-stimulating factor 1 receptor by CRISPR/Cas9 affects metabolism and locomotion capacity. Biochemical and Biophysical Research Communications, 2021, 551, 93-99.	2.1	6
11	Biodegradable BiOCl platform for oxidative stress injury–enhanced chemodynamic/radiation therapy of hypoxic tumors. Acta Biomaterialia, 2021, 129, 280-292.	8.3	39
12	Tumor Microenvironment Modulation Platform Based on Composite Biodegradable Bismuth–Manganese Radiosensitizer for Inhibiting Radioresistant Hypoxic Tumors. Small, 2021, 17, e2101015.	10.0	38
13	Intraperitoneal Injection of Cyanine-Based Nanomicelles for Enhanced Near-Infrared Fluorescence Imaging and Surgical Navigation in Abdominal Tumors. ACS Applied Bio Materials, 2021, 4, 5695-5706.	4.6	8
14	Electrostatic self-assembled Iridium(III) nano-photosensitizer for selectively disintegrated and mitochondria targeted photodynamic therapy. Dyes and Pigments, 2020, 175, 108105.	3.7	20
15	<p>Celecoxib Exerts a Therapeutic Effect Against Demyelination by Improving the Immune and Inflammatory Microenvironments</p> . Journal of Inflammation Research, 2020, Volume 13, 1043-1055.	3.5	5
16	Functionalization of bismuth sulfide nanomaterials for their application in cancer theranostics. Chinese Chemical Letters, 2020, 31, 3015-3026.	9.0	20
17	A heteropolysaccharide purified from leaves of Ilex latifolia displaying immunomodulatory activity in vitro and in vivo. Carbohydrate Polymers, 2020, 245, 116469.	10.2	26
18	Mesoporous Bi-Containing Radiosensitizer Loading with DOX to Repolarize Tumor-Associated Macrophages and Elicit Immunogenic Tumor Cell Death to Inhibit Tumor Progression. ACS Applied Materials & Interfaces, 2020, 12, 31225-31234.	8.0	24

Υυμαο Li, æŽέ'°çš"

#	Article	IF	CITATIONS
19	PEGylated iridium-based nano-micelle: Self-assembly, selective tumor fluorescence imaging and photodynamic therapy. Dyes and Pigments, 2020, 182, 108651.	3.7	16
20	Folic acid-nanoscale gadolinium-porphyrin metal-organic frameworks: fluorescence and magnetic resonance dual-modality imaging and photodynamic therapy in hepatocellular carcinoma. International Journal of Nanomedicine, 2019, Volume 14, 57-74.	6.7	35
21	Ultrafast Synthesizing Bismuth Mesoporous Nanolitchi Radiosensitizer Loading High Dose DOX for CT-Guided Enhanced Chemoradiotherapy. ACS Applied Materials & Interfaces, 2019, 11, 42932-42942.	8.0	34
22	ldentification and evaluation of antivirals for Rift Valley fever virus. Veterinary Microbiology, 2019, 230, 110-116.	1.9	10
23	A near-infrared frequency upconversion probe for nitroreductase detection and hypoxia tumor in vivo imaging. Sensors and Actuators B: Chemical, 2019, 286, 337-345.	7.8	33
24	Ultrafast synthesis of fluorine-18 doped bismuth based upconversion nanophosphors for tri-modal CT/PET/UCL imaging <i>in vivo</i> . Chemical Communications, 2019, 55, 7259-7262.	4.1	18
25	An AEE-active probe combined with cyanoacrylate fuming for a high resolution fingermark optical detection. Sensors and Actuators B: Chemical, 2019, 283, 99-106.	7.8	14
26	An AIPE-active heteroleptic Ir(III) complex for latent fingermarks detection. Sensors and Actuators B: Chemical, 2018, 259, 840-846.	7.8	30
27	Potent anticancer activity of a new bismuth (III) complex against human lung cancer cells. Journal of Inorganic Biochemistry, 2017, 168, 18-26.	3.5	28
28	SiO 2 encapsulated nanofluorophor: Photophysical properties, aggregation induced emission and its application for cell mitochondria imaging. Dyes and Pigments, 2017, 139, 110-117.	3.7	10
29	A cation-exchange controlled core–shell MnS@Bi ₂ S ₃ theranostic platform for multimodal imaging guided radiation therapy with hyperthermia boost. Nanoscale, 2017, 9, 14364-14375.	5.6	53
30	Down-regulation of interleukin 7 receptor (IL-7R) contributes to central nervous system demyelination. Oncotarget, 2017, 8, 28395-28407.	1.8	9
31	Effects of PB1-F2 on the pathogenicity of H1N1 swine influenza virus in mice and pigs. Journal of General Virology, 2017, 98, 31-42.	2.9	9
32	Pathogenicity of modified bat influenza virus with different M genes and its reassortment potential with swine influenza A virus. Journal of General Virology, 2017, 98, 577-584.	2.9	15
33	elF3i activity is critical for endothelial cells in tumor induced angiogenesis through regulating VEGFR and ERK translation. Oncotarget, 2017, 8, 19968-19979.	1.8	9
34	Effects of copper oxide nanoparticles on developing zebrafish embryos and larvae. International Journal of Nanomedicine, 2016, 11, 905.	6.7	52
35	Mouse model for the Rift Valley fever virus MP12 strain infection. Veterinary Microbiology, 2016, 195, 70-77.	1.9	14
36	AIE-active Ir(<scp>iii</scp>) complexes with tunable emissions, mechanoluminescence and their application for data security protection. Journal of Materials Chemistry C, 2016, 4, 2553-2559.	5.5	54

Υυμαο Li, æŽέ'°çš"

#	Article	IF	CITATIONS
37	Influence of a Naphthaldiimide Substituent at the Diimine Ligand on the Photophysics and Reverse Saturable Absorption of Pt ^{II} Diimine Complexes and Cationic Ir ^{III} Complexes. European Journal of Inorganic Chemistry, 2015, 2015, 5241-5253.	2.0	11
38	Ratiometric Monitoring of Intracellular Drug Release by an Upconversion Drug Delivery Nanosystem. ACS Applied Materials & Interfaces, 2015, 7, 12278-12286.	8.0	57
39	Aza-boron-diquinomethene complexes bearing N-aryl chromophores: synthesis, crystal structures, tunable photophysics, the protonation effect and their application as pH sensors. Journal of Materials Chemistry C, 2015, 3, 3774-3782.	5.5	20
40	A novel model of demyelination and remyelination in a GFP-transgenic zebrafish. Biology Open, 2015, 4, 62-68.	1.2	25
41	Ultrasensitive Near-Infrared Fluorescence-Enhanced Probe for <i>in Vivo</i> Nitroreductase Imaging. Journal of the American Chemical Society, 2015, 137, 6407-6416.	13.7	408
42	The MYC, TERT, and ZIC1 Genes Are Common Targets of Viral Integration and Transcriptional Deregulation in Avian Leukosis Virus Subgroup J-Induced Myeloid Leukosis. Journal of Virology, 2014, 88, 3182-3191.	3.4	23
43	Synthesis and photophysics of reverse saturable absorbing heteroleptic iridium(<scp>iii</scp>) complexes bearing 2-(7-R-fluoren-2′-yl)pyridine ligands. Dalton Transactions, 2014, 43, 1724-1735.	3.3	23
44	An AIE-active boron-difluoride complex: multi-stimuli-responsive fluorescence and application in data security protection. Chemical Communications, 2014, 50, 12951-12954.	4.1	183
45	The Translation Initiation Factor eIF3i Up-regulates Vascular Endothelial Growth Factor A, Accelerates Cell Proliferation, and Promotes Angiogenesis in Embryonic Development and Tumorigenesis. Journal of Biological Chemistry, 2014, 289, 28310-28323.	3.4	24
46	Pt(II) Bipyridyl Complexes Bearing Substituted Fluorenyl Motif on the Bipyridyl and Acetylide Ligands: Synthesis, Photophysics, and Reverse Saturable Absorption. Inorganic Chemistry, 2014, 53, 9516-9530.	4.0	21
47	Influence of Different Diimine (N ^{â^§} N) Ligands on the Photophysics and Reverse Saturable Absorption of Heteroleptic Cationic Iridium(III) Complexes Bearing Cyclometalating 2-{3-[7-(Benzothiazol-2-yl)fluoren-2-yl]phenyl}pyridine (C ^{â^§} N) Ligands. Journal of Physical Chemistry C, 2014, 118, 23233-23246.	3.1	40
48	Synthesis and luminescent properties of star-burst D-Ï€-A compounds based on 1,3,5-triazine core and carbazole end-capped phenylene ethynylene arms. Journal of Luminescence, 2014, 156, 130-136.	3.1	14
49	Effects of Extended Ï€-Conjugation in Phenanthroline (N ^{â^§} N) and Phenylpyridine (C ^{â^§} N) Ligands on the Photophysics and Reverse Saturable Absorption of Cationic Heteroleptic Iridium(III) Complexes. Journal of Physical Chemistry C, 2014, 118, 6372-6384.	3.1	58
50	A bioprobe based on aggregation induced emission (AIE) for cell membrane tracking. Chemical Communications, 2013, 49, 11335.	4.1	122
51	Pt(<scp>ii</scp>) diimine complexes bearing carbazolyl-capped acetylide ligands: synthesis, tunable photophysics and nonlinear absorption. Dalton Transactions, 2013, 42, 160-171.	3.3	25
52	Long-Lived π-Shape Platinum(II) Diimine Complexes Bearing 7-Benzothiazolylfluoren-2-yl Motif on the Bipyridine and Acetylide Ligands: Admixing Ï€,Ĩ€* and Charge-Transfer Configurations. Journal of Physical Chemistry C, 2013, 117, 5908-5918.	3.1	33
53	Synthesis, photophysics and reverse saturable absorption of bipyridyl platinum(ii) bis(arylfluorenylacetylide) complexes. Dalton Transactions, 2013, 42, 4398.	3.3	34
54	Isolation, identification, and phylogenetic analysis of two avian leukosis virus subgroup J strains associated with hemangioma and myeloid leukosis. Veterinary Microbiology, 2013, 166, 356-364.	1.9	32

Υυμαο Li, æŽέ'°çš"

#	Article	IF	CITATIONS
55	Synthesis, insecticidal activity, and structure–activity relationship (SAR) of anthranilic diamides analogs containing oxadiazole rings. Organic and Biomolecular Chemistry, 2013, 11, 3979.	2.8	47
56	Nonlinear Absorbing Cationic Iridium(III) Complexes Bearing Benzothiazolylfluorene Motif on the Bipyridine (Nâ^§N) Ligand: Synthesis, Photophysics and Reverse Saturable Absorption. ACS Applied Materials & Interfaces, 2013, 5, 6556-6570.	8.0	50
57	Tuning Photophysical Properties and Improving Nonlinear Absorption of Pt(II) Diimine Complexes with Extended l̃€-Conjugation in the Acetylide Ligands. Journal of Physical Chemistry A, 2013, 117, 1907-1917.	2.5	37
58	Long-lived platinum(ii) diimine complexes with broadband excited-state absorption: efficient nonlinear absorbing materials. Dalton Transactions, 2012, 41, 12353.	3.3	34
59	Photophysics and nonlinear absorption of 4,4′-diethynylazobenzene derivatives terminally capped with substituted aromatic rings. Journal of Photochemistry and Photobiology A: Chemistry, 2012, 239, 47-54.	3.9	5
60	The role of microglia in the neurogenesis of zebrafish retina. Biochemical and Biophysical Research Communications, 2012, 421, 214-220.	2.1	56
61	Phenylene ethynylene azobenzenes with symmetrical peripheral chromophores: Synthesis, optical properties and photoisomerization behaviors study. Dyes and Pigments, 2012, 92, 626-632.	3.7	9
62	Nonlinear Absorbing Platinum(II) Diimine Complexes: Synthesis, Photophysics, and Reverse Saturable Absorption. Chemistry - A European Journal, 2012, 18, 11440-11448.	3.3	34
63	Synthesis and luminescent properties of carbazole end-capped phenylene ethynylene compounds. Journal of Luminescence, 2012, 132, 191-197.	3.1	11
64	The synthesis, crystal structure and photophysical properties of mononuclear platinum(II) 6-phenyl-[2,2′]bipyridinyl acetylide complexes. Dyes and Pigments, 2011, 88, 88-94.	3.7	13
65	Synthesis, Crystal Structure and Fungicidal Activities of New Type Oxazolidinone-Based Strobilurin Analogues. Bulletin of the Korean Chemical Society, 2010, 31, 3341-3347.	1.9	23
66	Synthesis, optical properties and crystal structures of carbazole end-capped phenylene ethynylene blue light-emitting materials. Journal of Luminescence, 2010, 130, 1183-1188.	3.1	4
67	Photophysics and Nonlinear Absorption of Cyclometalated 4,6-Diphenyl-2,2′-bipyridyl Platinum(II) Complexes with Different Acetylide Ligands. Journal of Physical Chemistry A, 2010, 114, 12639-12645.	2.5	42